Australas Phys Eng Sci Med (2014) 37:731–742
DOI 10.1007/s13246-014-0310-9

SCIENTIFIC PAPER

Evaluation of respiratory pattern during respiratory-gated radiotherapy

Suguru Dobashi · Shinichiro Mori

Received: 25 December 2013 / Accepted: 29 October 2014 / Published online: 22 November 2014

Abstract The respiratory cycle is not strictly regular, and generally varies in amplitude and period from one cycle to the next. We evaluated the characteristics of respiratory patterns acquired during respiratory gating treatment in more than 300 patients. A total 331 patients treated with respiratory-gated carbon-ion beam therapy were selected from a group of patients with thoracic and abdominal conditions. Respiratory data were acquired for a total of 3,171 fractions using an external respiratory sensing monitor and evaluated for respiratory cycle, duty cycle, magnitude of baseline drift, and intrafractional/interfractional peak inhalation/exhalation positional variation. Results for the treated anatomical sites and patient positioning were compared. Mean ± SD res

piratory cycle averaged over all patients was 4.1 ± 1.3 s. Mean ± SD duty cycle averaged over all patients was 36.5 ± 7.3 %. Two types of baseline drift were seen, the first decremental and the second incremental. For respiratory peak variation, the mean intrafractional variation in peak-inhalation position relative to the amplitude in the first respiratory cycle (15.5 ± 9.3 %) was significantly larger than that in exhalation (7.5 ± 4.6 %). Interfractional variations in inhalation (17.2 ± 18.5 %) were also significantly greater than those in exhalation (9.4 ± 10.0 %). Statistically significant differences were observed between patients in the supine position and those in the prone position in mean respiratory cycle, duty cycle, and intra-/interfractional variations. We quantified the characteristics of the respiratory curve based on a large number of respiratory data obtained during treatment. These results might be useful in improving the accuracy of respiratory-gated treatment.

Keywords Carbon-ion beam · Gating · Respiration · Intrafractional · Interfractional

S. Dobashi · S. Mori (✉)
Research Center for Charged Particle Therapy, National Institute of Radiological Sciences, Inage-Ku, Chiba 263-8555, Japan
e-mail: shinshin@nirs.go.jp

S. Dobashi
Department of Health Sciences, Tohoku University Graduate School of Medicine, Sendai, Japan

Introduction

While radiotherapy techniques have greatly improved over the last several years, as exemplified by intensity-modulated radiotherapy (IMRT), dynamic arc therapy in photon beam therapy, and layer-stacking and scanning irradiation in particle beam therapy, several uncertainties which decrease treatment accuracy remain. Among these, respiratory motion is clearly the most important, because a tumor does not receive an adequate dose when it moves outside the planning target volume due to respiration. Respiratory motion primarily affects two factors, dose distribution (dose blurring effects, over-/undershoot etc.) [1–5] and the quality of imaging (distortions of organ shape in 4DCT for treatment plan) [6]. These factors combine to degrade the accuracy of treatment in the thoracic and abdominal regions.

As a strategy to compensate for respiratory motion which is applicable to large groups of patients, several treatment centers have implemented respiratory-gating techniques under free-breathing conditions. Respiratory gating is more feasible than voluntary or imposed breath-holding techniques [7], since breath-holding cannot be tolerated by patients with compromised respiratory function. Respiratory gating is also preferable in that the devices required for this method can be more easily and

inexpensively integrated into treatment machinery than those required for other motion compensation techniques, such as dynamic multi-leaf tracking [8, 9], the moving couch method [10], tumor tracking with fluoroscopy [11, 12], and robotic control of the linear accelerator [13].

Dose conformation is particularly important in carbon-ion beam therapy. Our center has performed passive carbon-ion beam therapy for more than 15 years, and successfully began carbon-ion beam scanning treatment in the second quarter of 2011 [14]. Dose conformation with scanning irradiation can be degraded by interplay effects between respiratory motion and beam-scanning [15, 16]. One approach to improving dose conformity is the use of a rescan technique [17]. We extended this idea to develop the phase-control rescan technique, which irradiates the carbon-ion beam several times during the gating window [3]. Respiratory-gated passive irradiation with an external respiratory sensing monitor has been routinely performed since 1996 [18], but respiratory-gated scanning irradiation has yet to be implemented. Successful completion of treatment requires that the respiratory pattern is stable and reproducible, particularly in scanning treatment with a high dose concentration.

To assess and minimize the influence of respiratory motion on dose conformation it is necessary to properly quantify the characteristics of the respiratory pattern and its degree of variation. Several authors have investigated these factors. Basic characteristics of respiratory motion were summarized by Keall, Mageras, Balter [19]. The stability and reproducibility of respiratory pattern have been analyzed based on the motion of external markers or internal fiducials [20–23]. One characteristic respiratory pattern to be considered during treatment is baseline drift, which can drastically degrade dose conformity, particularly in radiotherapy over an extended treatment time, such as in Cyberknife lung stereotactic body radiation therapy (SBRT) [24]. We should also note that respiratory pattern for the same patient varies not only during a treatment but also between treatments [2]. Furthermore, although some studies have reported a good correlation between the motion of external markers and that of internal tumors or the diaphragm [25–27], detailed examinations have revealed that these in fact differ [28–33].

While several authors have quantified the characteristics of and variation in respiratory pattern during a treatment, as well as the relation between external marker motion and internal tumor motion, these studies were based on data from several to several tens of patients. Fundamental information on respiratory pattern and its degree of variation obtained by statistical analysis of external marker motion in a large number of patients should allow improvements in the accuracy of respiratory gating treatment.

Here, we quantified the characteristics of respiratory pattern based on wave form data from more than 300 patients acquired from the motion of the external marker during respiratory gating treatment. We also used this large amount of data to perform subgroup analysis of respiratory characteristics (respiratory cycle, duty cycle, and intra-/interfractional variation) with regard to treatment anatomical site and patient position.

Materials and methods

Patients and data acquisition

A total of 331 patients (mean age: 66.8 years, S.D.: ± 14.8 years) treated with respiratory-gated carbon-ion beam treatment were randomly selected from a group of patients with conditions involving the lung, liver, rectum, pancreas, B&S (bone and soft tissue sacral chordoma), lymph node, esophagus, and uterus (Table 1). Respiratory data were obtained for a total of 3,171 fractions in all patients (supine, 1172; prone, 1999). Carbon-ion beam treatment for these anatomical sites in our institute is performed under free-breathing conditions and the patients are fixed by low-temperature thermoplastic immobilization shell (Shellfitter; Kuraray Co., Ltd., Osaka, Japan) and hydraulic urethane resin basement (Moldcare; Alcare, Tokyo, Japan). The thermoplastic device is molded by softening the shell above 45 C and fitting it to the patient's body so that it covers the upper half of the patient's body [37]. In our center, basically all patients with tumors in the anatomical sites which may be affected by respiratory motion are treated in the respiratory gated treatment. There was, therefore, no threshold value in selecting patients as for the amplitude of the respiratory motion.

Respiratory curves were acquired from the motion of the patient body surface using a respiratory sensing monitor, which consisted of a position-sensitive detector (PSD) sensor and infrared-emitting source on the patient's body (Toyonaka Lab, Osaka, Japan) [34]. The PSD camera was mounted on the treatment couch around the feet of a patient and detected the motion of the infrared-emitting device. The wave form was amplified by a zoom lens of the camera so that we can identify the respiratory peaks. The location of the infrared-emitting device set on the patient surface was chosen so that the emitting device did not interfere with the treatment beam and remained unchanged throughout a course of treatments. The details of the respiratory monitoring system used in NIRS have been reported by Minohara et al. [18].

The respiratory curve and gating window were recorded at a sampling time of 5 ms. Irradiation with the treatment beam was delivered only when the respiratory curve was under the threshold (gating window). We defined the duty cycle as the ratio of time when the respiratory curve was under the gating window to that of the whole respiratory

Table 1 Patient list and treatment time per fraction

Anatomical site	Age (y)		No. pt	No. resp. data	Treatment time/fr. (S)	
	Mean	SD	Total (Supine, Prone)	Total (Supine, Prone)	Mean (Supine, Prone)	SD (Supine, Prone)
Lung	76.7	9.7	85 (38, 57)	516 (245, 271)	90 (92, 91)	37 (33, 41)
Liver	69.3	10.6	61 (33, 32)	209 (99, 110)	141 (160, 119)	83 (94, 61)
Rectum	60.8	12.1	44 (11, 42)	628 (74, 554)	74 (85, 74)	21 (39, 20)
Pancreas	66.0	9.8	26 (26, 25)	236 (169, 67)	76 (75, 78)	15 (15, 29)
B&S	59.3	18.2	93 (50, 85)	1336 (412, 924)	94 (101, 98)	34 (40, 37)
Lymph node	61.7	9.8	10 (10, 8)	79 (52, 27)	59 (59, 53)	22 (22, 21)
Esophagus	66.7	5.1	7 (7, 7)	56 (28, 28)	84 (83, 86)	21 (34, 24)
Uterus	67.9	14.2	7 (6, 4)	111 (93, 18)	78 (72, 81)	21 (15, 32)
Total	66.8	14.8	33 (181, 258)	3171 (1172, 1999)	96 (101, 92)	50 (58, 40)

No. pt. number of patients, *B&S* bone and soft tissue, *SD* standard deviation, *resp.* respiratory, *fr* fraction

cycle. The gating window was set around peak exhalation to maintain an approximately 30 % duty cycle in each cycle. When the respiratory curve varied during a treatment, the therapist manually adjusted the gating window to maintain the original duty cycle. In this procedure it is assumed that the discrepancy between the external surrogate motion and the internal tumor motion is small enough to be compensated for by the margin in the planning target volume [18].

Data analysis

We quantified four metrics using these respiratory curve data, namely (i) respiratory cycle, (ii) duty cycle, (iii) magnitude of baseline drift, and (iv) intrafractional/interfractional respiratory pattern variation.

Characteristics of the respiratory curve were defined based on respiratory peak position. To identify the peaks, we first calculated a 4-s moving average of the amplitude, and then identified the exhalation/inhalation peaks as the minimum/maximum point in each region segmented by the average amplitude. To reduce the effect of signal noise, such as coughs or hiccups, we removed pairs of peaks which were too close together from the points thus identified; in other words, if either the time difference between adjacent exhalation and inhalation points was less than 0.4 s or their amplitude difference was less than 40 % of the standard deviation of the set of distances between all adjacent exhalation/inhalation pairs in the fraction, we deleted the pair of peaks. The validity of this criterion was confirmed by checking that peaks with an obviously smaller amplitude or respiratory cycle than others were properly removed. Based on this criterion, 95 % of the respiratory curves contained no invalid peaks, 4 % contained less than 5, and the remaining 1 % contained 5–43. We analyzed only the respiratory data that were obtained between the first irradiation and the last irradiation in each treatment fraction. Since the respiratory sensing monitor provides the relative position of the surface marker only, we normalized the respiratory amplitude by the amplitude of the first respiratory cycle in each fraction as identified following the procedure above. We dropped respiratory data with fewer than 10 respiratory cycles from the analysis to reduce statistical error arising from data with few respiratory cycles (71 fractions in 3,242 were dropped).

Respiratory cycle

A respiratory cycle was defined as the time between a peak exhalation and the next peak exhalation (Fig. 1a). We denote the respiratory cycle as $T = (t_k, fr_m, pt_n)$,where t_k is the time of the k-th exhalation peak, and fr_m and pt_n are the fraction number and patient number, respectively. The respiratory cycle for patient pt_n was calculated by first averaging all respiratory cycles in each fraction and then averaging these results over all fractions:

$$T(\bar{t}, \overline{fr}, pt_n) = \frac{1}{M_n}\sum_{m=1}^{M_n}\frac{1}{K_{n,m}}\sum_{k=1}^{K_{n,m}} T(t_k, fr_m, pt_n),$$

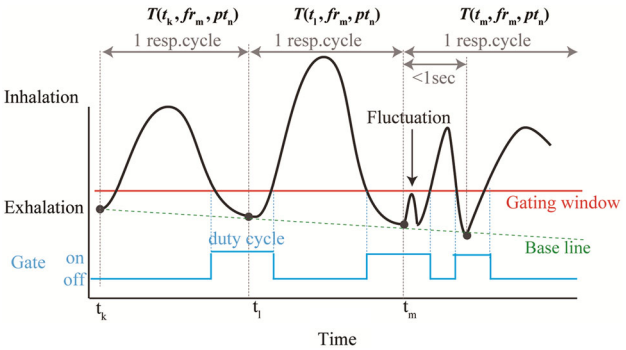

Fig. 1 Definitions of respiratory cycle, duty cycle, gating window, and base line

where $K_{n,m}$ and M_n are the total number of respiratory cycles in the m-th fraction of patient n and the total number of fractions for patient n, respectively.

Duty cycle

Duty cycle was defined as the ratio of the beam-on treatment time to the total treatment time [35]. We set the gating window to the amplitude under which the treatment beam is irradiated (red line in Fig. 1a). Because our current respiratory gating method is phase-based, the therapist attempted to adjust the gating window to maintain the initial duty cycle in response to variations in respiratory pattern based on the therapist's own judgment. We calculated the time in which respiratory curves were under the gating window for each respiratory cycle, each fraction, and each patient $D(t_k, fr_m, pt_n)$ (light blue line in Fig. 1a) during the treatment, and then averaged these values in the same manner as for the respiratory cycle. The results were expressed as a percentage (%):

$$D(\bar{t},\overline{fr},pt_n) = \frac{1}{M_n}\sum_{m=1}^{M_n}\frac{1}{K_{n,m}}\sum_{k=1}^{K_{n,m}} D(t_k,fr_m,pt_n).$$

Magnitude of baseline drift

Baseline drift is a well-known phenomenon in which peak exhalation position gradually drifts in a particular direction (downward or upward) during treatment [24, 29, 33]. In this analysis, to assess the magnitude of baseline drift occurring during a typical treatment time, we analyzed only those fractions in which treatment lasted more than two minutes (571 fractions). The behavior of baseline drift during the two minutes from the first irradiation was assessed with regard to both global trend and variation during a treatment.

To assess for a global trend in baseline, we fit a linear function to the peak exhalation position using the least-squares method (dotted green line in Fig. 1a). We defined the magnitude of baseline drift by the slope value of the linear function expressed in units of percent-per-minute (= %/min). Since the respiratory curve was normalized by the amplitude of the first respiratory cycle in each fraction, the slope value gives the "averaged" variation of peak exhalation positions per minute relative to the amplitude of the first respiratory cycle. Negative and positive values show decreasing and increasing respiratory amplitude, respectively.

To analyze the variation in baseline in each fraction, following a procedure similar to that of Zhao et al. [24], we first averaged the peak exhalation positions in every 20-s block and assessed how the average peak exhalation positions (6 points in each fraction) were distributed during two minutes after the first irradiation. We took as the origin the average position in the first 20 s and assessed deviations of the average position in each time block from the origin.

Intrafractional/interfractional respiratory pattern variations

To quantify intrafractional and interfractional variation, we defined two types of standard deviation, as follows.

For intrafractional respiratory variation during a single fraction, we calculated the standard deviation of peak positions (either exhalation or inhalation) in each fraction:

$$SD_p(fr_m,pt_n) = \sqrt{\frac{1}{K_{n,m}-1}\sum_{k=1}^{K_{n,m}}\left(P(t_k,fr_m,pt_n)-\bar{P}_{n,m}\right)^2},$$

where $P(t_k, fr_m, pt_n)$ denotes the longitudinal position of the respiratory curve at either peak exhalation or peak inhalation, and $\bar{P}_{n,m}$ is the averaged value of $P(t_k, fr_m, pt_n)$ in terms of k for the m-th fraction of patient n. We measured the degree of intrafractional variation by the standard deviation in each fraction. For a particular patient, the intrafractional respiratory variation was defined by the mean standard deviation over all fractions:

$$V_{\text{intra}}(pt_n) = \frac{1}{M_n}\sum_{m=1}^{M_n} SD_p(fr_m,pt_n).$$

With regard to interfractional variation for patient n, we first calculated the mean peak posiexhalation was more stabletion (either exhalation or inhalation) in each fraction, and then the standard deviation for all fractions:

$$V_{\text{inter}}(pt_n) = \sqrt{\frac{1}{M_n-1}\sum_{m=1}^{M_n}\left(\bar{P}_{n,m}-\frac{1}{M_n}\sum_{m=1}^{M_n}\overline{P}_{n,m}\right)}.$$

Statistical analysis

For respiratory cycle and duty cycle, subgroup analysis was performed with regard to both anatomical site (eight sites: lung, liver, rectum, etc.) and patient position (supine/prone) using the Kruskal–Wallis two-way analysis of variance (ANOVA) method, with significance level set at $p = 0.05$.

For the slope value of baseline drift, due to the small number of fractions, we did not perform subgroup analysis by anatomical site. When we assessed statistically significant differences between two groups, we first confirmed the normality of the distribution using the Kolmogorov–Smirnov test. If the null hypothesis that the data has a standard normal distribution was not rejected, the two groups were compared using Student's t test; otherwise,

they were compared using the Wilcoxon test. Significance level was set at $p = 0.05$.

All statistical analyses were performed using Matlab R2012a (MathWorks, Natick, MA).

Results

Respiratory cycle

The statistics of respiratory cycle are summarized in Table 2. Mean ± SD respiratory cycle averaged over all patients was 4.1 ± 1.3 s. Maximum respiratory cycle was 13.6 s (liver case). The number of patients with a mean respiratory cycle of greater than 10 s was 20. A histogram of duty cycle is shown in Fig. 2a.

Subgroup analysis of respiratory cycle was performed using two-way ANOVA with regard to treatment anatomical site and patient position. A statistically significant difference was observed between patients in the supine (= 4.3 ± 1.6 s) and prone positions (= 3.9 ± 1.2 s). Among anatomical treatment sites, a statistically significant difference was observed only between lung (= 3.6 ± 0.9 s) and liver (= 4.6 ± 2.1 s).

Duty cycle

Mean ± SD duty cycle averaged over all patients was 36.5 ± 7.3 %. Maximum and minimum duty cycles were 58.2 and 14.5 %, respectively. A histogram of duty cycle is shown in Fig. 2b, and the results are summarized in Table 2.

The duty cycle significantly differed between patients in the supine (= 36.6 ± 9.1 %) and prone positions (= 34.3 ± 7.8 %). The duty cycle of liver patients (= 41.8 ± 7.0 %) significantly differed from patients with cancers at other anatomical sites. The duty cycle of lung patients (= 37.1 ± 7.2 %) significantly differed from those of esophagus (= 29.1 ± 3.2 %), uterus (= 29.4 ± 4.9 %) and liver patients (= 41.8 ± 7.0 %). No statistically significant difference was observed between any other pair of anatomical sites.

Magnitude of baseline drift

Applying a linear fitting function to the exhalation points using the least-squares method, two types of baseline drift were observed, decremental baseline drift (Fig. 3a) and incremental baseline drift (Fig. 3b). Both examples show simple drift of the peak exhalation position as a linear function of time. In 321 of 576 curves (= 56 %), the slope value was significantly different from zero (*t* test, $p < 0.05$). Among these, 55 and 45 % showed decremental and incremental drift, respectively. The histogram of the determination coefficient (R^2) and the scatter plot between the R^2 and the slope value are given in Fig. 4a and b, respectively. In Fig. 4b, the R^2 values for high slope values (>50 %/min) are distributed in a region with relatively

Table 2 Summary of respiratory cycle (s) and duty cycle (%)

Metrics	Anatomical site	Mean value Total (Supine, Prone)	Standard deviation Total (Supine, Prone)	Median Total (Supine, Prone)	Maximum Total (Supine, Prone)	Minimum Total (Supine, Prone)
Respiratory cycle [sec]	Lung	3.6 (3.8, 3.6)	0.9 (1.1, 0.9)	3.4 (3.4, 3.5)	7.1 (7.0, 7.3)	2.1 (2.8, 2.1)
	Liver	4.6 (5.4, 4.1)	2.1 (2.7, 1.5)	4.0 (4.8, 3.8)	13.6 (13.6, 10.4)	2.4 (2.4, 2.6)
	Rectum	3.8 (3.9, 3.8)	0.9 (0.9, 0.9)	3.7 (3.9, 3.9)	7.0 (5.2, 7.0)	2.5 (2.9, 2.5)
	Pancreas	4.6 (4.8, 4.3)	1.2 (1.3, 1.1)	4.5 (4.6, 4.0)	7.4 (8.1, 7.0)	3.1 (3.2, 2.9)
	B&S	4.1 (4.2, 4.1)	1.2 (1.3, 1.5)	3.8 (3.9, 3.8)	7.9 (8.2, 11.7)	2.2 (2.2, 2.4)
	Lymph node	3.9 (4.0, 3.8)	0.9 (1.1, 0.9)	3.4 (3.4, 3.4)	5.5 (6.3, 5.5)	3.1 (3.1, 3.0)
	Esophagus	3.9 (4.0, 3.8)	1.0 (1.0, 1.0)	3.8 (4.0, 3.6)	5.6 (5.3, 5.8)	2.6 (2.6, 2.5)
	Uterus	3.8 (3.5, 3.9)	1.0 (0.7, 1.3)	3.5 (3.4, 3.6)	5.7 (4.7, 5.7)	2.6 (2.5, 2.6)
	Total	4.1 (4.3, 3.9)	1.3 (1.6, 1.2)	3.7 (3.9, 3.7)	13.6 (13.6, 5.7)	2.1 (2.2, 2.1)
Duty cycle [%]	Lung	37.1 (35.1, 37.3)	7.2 (7.3, 7.6)	38.3 (36.1, 38.3)	51.3 (48.4, 51.3)	14.5 (17.8, 14.5)
	Liver	41.8 (42.4, 40.8)	7.0 (8.5, 5.6)	41.1 (40.8, 41.1)	58.2 (58.2, 48.8)	17.8 (17.8, 20.5)
	Rectum	36.0 (35.9, 35.2)	7.5 (9.5, 6.1)	35.2 (33.9, 35.2)	51.2 (49.3, 51.2)	25.4 (21.1, 22.7)
	Pancreas	36.0 (39.2, 28.1)	7.2 (8.0, 6.2)	35.2 (38.0, 29.3)	50.7 (54.6, 40.1)	26.0 (27.6, 13.1)
	B&S	34.2 (33.8, 32.9)	6.6 (9.4, 7.6)	34.0 (34.5, 32.3)	53.7 (51.5, 54.6)	21.1 (15.0, 13.7)
	Lymph node	34.3 (37.6, 28.0)	8.9 (11.4, 5.2)	33.8 (38.4, 26.8)	45.4 (54.0, 37.4)	21.8 (20.9, 21.8)
	Esophagus	29.1 (29.9, 28.3)	3.2 (5.8, 3.9)	27.7 (29.9, 26.7)	34.0 (38.5, 34.0)	24.9 (20.9, 23.2)
	Uterus	29.4 (32.3, 23.3)	4.9 (5.8, 1.0)	29.6 (31.5, 23.5)	37.0 (43.1, 24.3)	21.9 (25.8, 21.9)
	Total	36.5 (36.6, 34.3)	7.3 (9.1, 7.8)	35.9 (36.5, 34.0)	58.2 (58.2, 54.6)	14.5 (15.0, 13.1)

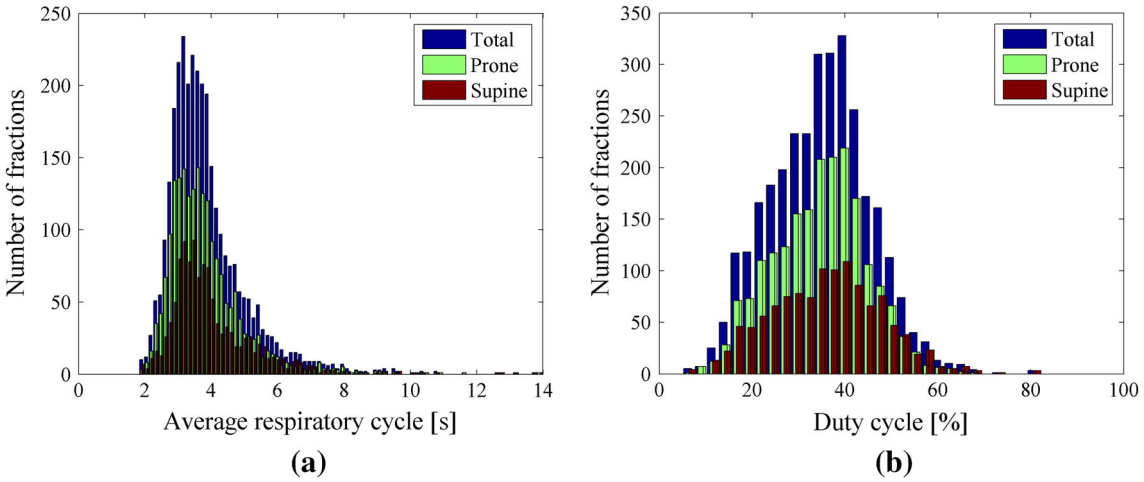

Fig. 2 **a** Histogram of mean respiratory cycle. **b** Histogram of mean duty cycle

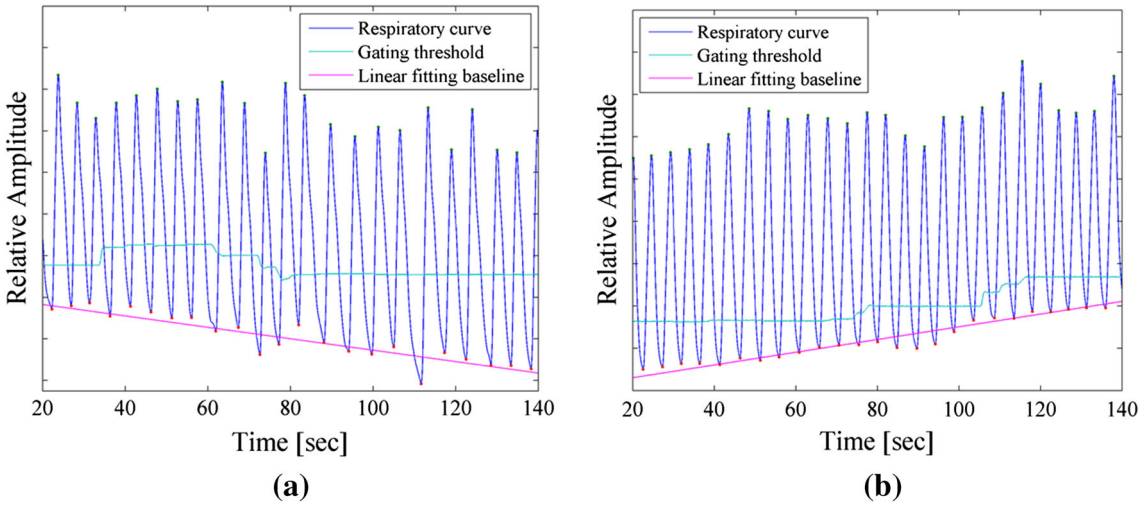

Fig. 3 **a** Example of respiratory data with a decremental baseline drift (= −16.7 %/min). Gating threshold and linear fitting function are shown in *light blue* and *red lines*, respectively. **b** Example of respiratory data with an incremental baseline drift (= 17.1 %/min)

high R^2 (>0.5), while for relatively low slope values (<30 %/min), the R^2 values are spread over a wide range, indicating that the peak exhalation position was not necessarily well fitted to a straight line. For the slope value, no statistical significant difference was observed between patients in the supine and prone positions.

The distribution of peak exhalation position averaged in every 20-s block in each fraction is plotted in Fig. 5. In this figure, we took the average position in the first 20 s as the origin of the baseline in each fraction. For all fractions investigated, each time block contained at least one exhalation peak (mean: 5.0 peaks, SD: 1.5, range: 1–30). The range of variation in each time block increased with time while the mean position remained at almost zero. Of 576 respiratory curves, 16 curves monotonously increased and 15 curves monotonously decreased. The mean ± SD of R^2 for the monotonously increasing curves and that for the monotonously decreasing curves were 0.76 ± 0.14 (range, 0.42–0.94) and 0.72 ± 0.21 (range, 0.28–0.92), respectively, showing relatively high correlation.

Correlation between baseline and gating threshold

The correlation between baseline and gating threshold was investigated. We calculated Pearson's correlation coefficient between peak exhalation position and gating level at the time of peak exhalation. The result is depicted in Fig. 6. Correlation coefficients of more than 0.5 were observed in 32.9 % of fractions, and negative correlation coefficients in 24.5 %. In respiratory gating treatment in our institute, gating threshold is adjusted by a therapist according to the change in respiratory pattern. However, when the peak exhalation position fluctuates only slightly around the first position of the treatment, the therapist does not attempt to

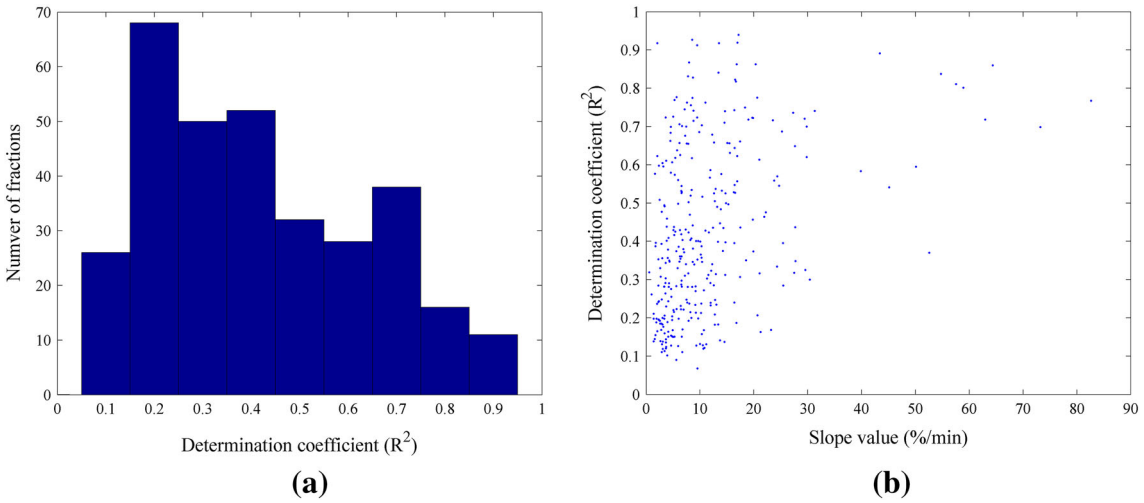

Fig. 4 **a** Histogram of the determination coefficient (R^2) for the linear function fitted to peak exhalation position. **b** *Scatter plot* between the slope value of the fitted linear function (%/min) and the determination coefficient

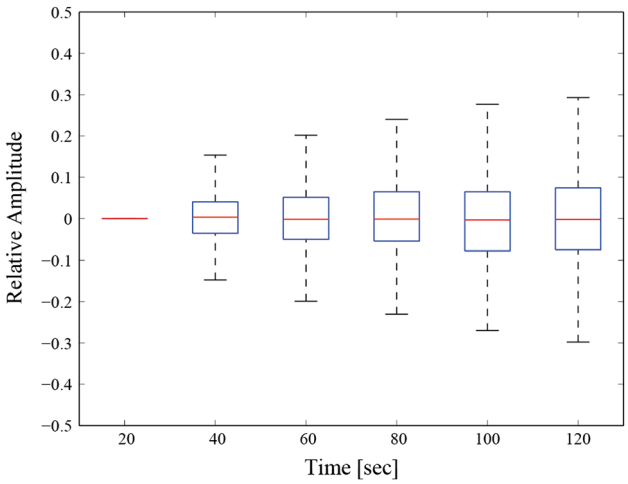

Fig. 5 Distribution of peak exhalation positions averaged in every 20-s block for patients whose treatment lasted more than 2 min. In the *box*-and-*whisker plot*, the central mark is the median, the edges of the *box* are the 25th and 75th percentiles, and the width of the whisker is chosen as four times the difference between the 25th and 75th percentiles. *Values* which lie outside the whisker are omitted

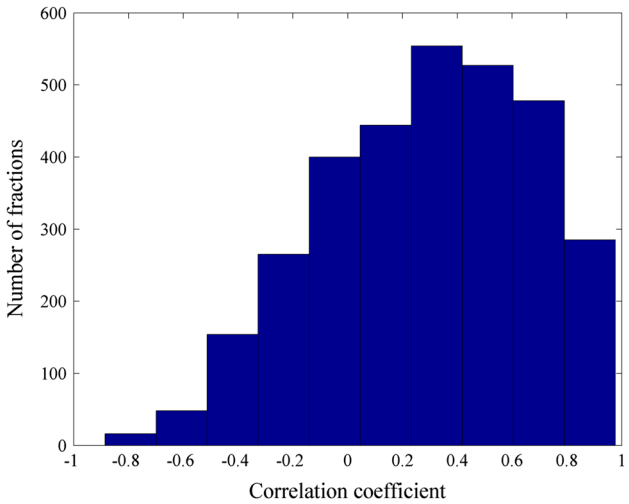

Fig. 6 Histogram of correlation coefficients between peak exhalation position and the level of the gating threshold at peak exhalation

change threshold level. The correlation can be negative in situations where the peak exhalation position fluctuates by a small amount while the gating threshold remains almost constant.

Intrafractional/interfractional respiratory pattern variations

An example of respiratory curves during the treatment course for a single patient (bone and soft tissue sacral chordoma case) is shown in Fig. 7. The respiratory pattern was largely stable during the first fraction. However, it varied in other fractions, particularly in peak inhalation position. Peak exhalation positions fluctuated as a function of time in fractions 3, 4 and 11. Intrafractional respiratory variation averaged over all fractions in this patient were 45.5 and 11.6 % for inhalation and exhalation, respectively, while interfractional variations were 47.6 and 18.9 %, respectively.

The histograms of intrafractional variation are given in Fig. 8a, b (inhalation and exhalation), and those of interfractional variation in Fig. 8c and d (inhalation and exhalation). Table 3 shows the mean ± SD of intrafractional and interfractional respiratory variations. In both cases, the variation in respiratory pattern in exhalation (Fig. 8b, d) is significantly smaller than that in inhalation (Fig. 8a, c) (Wilcoxon test, $p < 0.05$), indicating that exhalation was more stable than inhalation in both cases. In exhalation

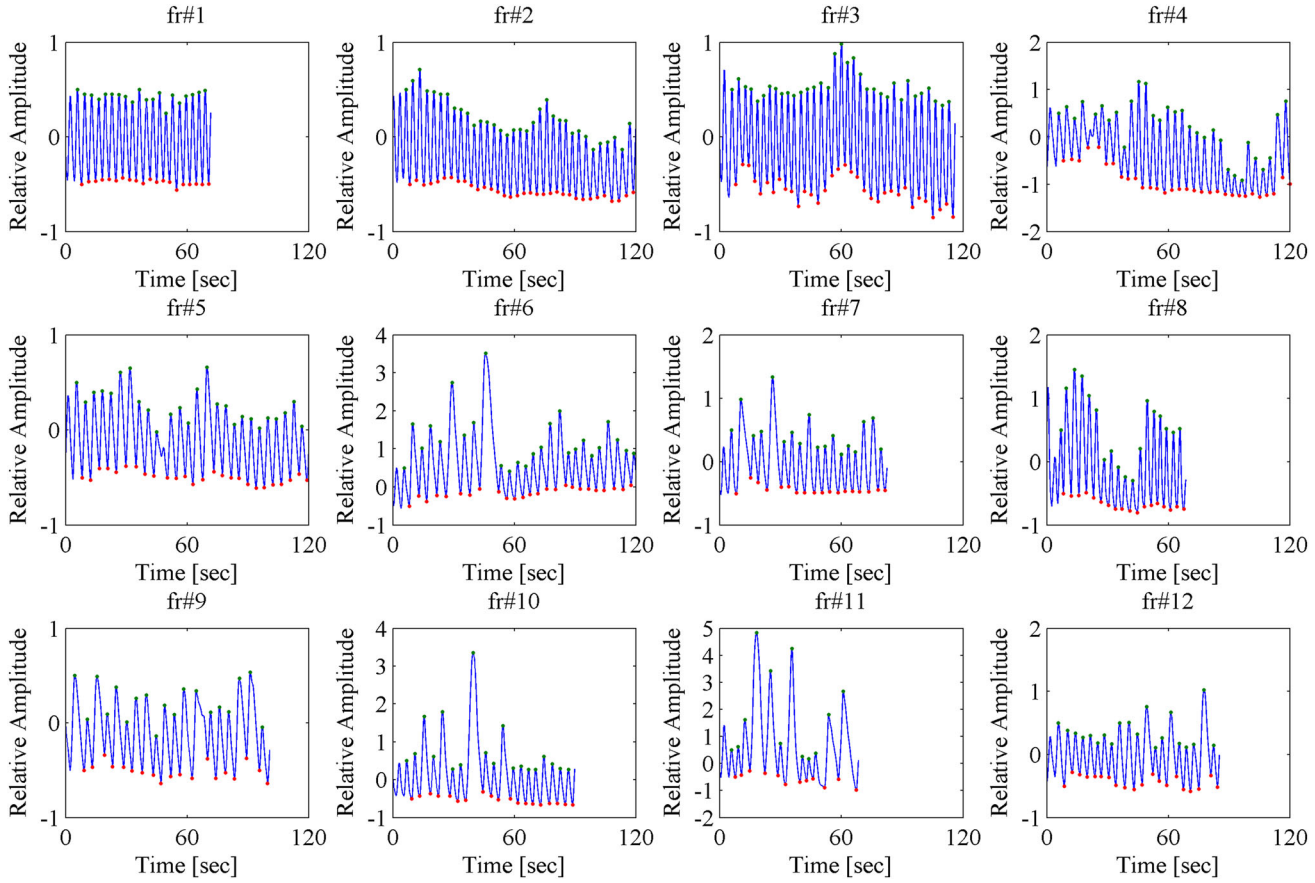

Fig. 7 Examples of respiratory curves during treatment course (12 fractions) in the same patient (bone and soft tissue sacral chordoma case)

(Fig. 8b, d), the intrafractional variation (Fig. 8b) was significantly smaller than interfractional variation (Fig. 8d) (Wilcoxon test, $p < 0.05$); while in inhalation (Fig. 8a, c), the intrafractional and interfractional variation did not differ significantly (Wilcoxon test, $p > 0.05$). In all cases, the magnitude of variation in the prone position was significantly smaller than that in the supine position (Wilcoxon, $p < 0.05$), indicating that the prone position was more stable than the supine position.

The degree of intrafractional variation (at exhalation) as a function of fraction number is depicted in Fig. 9 for patients treated in 12 fractions. No statistical significant difference was observed between intrafractional variation in the first fraction and that in the last (Wilcoxon, $p > 0.05$). The same is true for any other patient group with other total fraction numbers. This result indicates that the degree of the intrafractional variation did not necessarily decrease as treatment proceeded.

Discussion

We quantified the characteristics of respiration and its degree of variation in a large group of patients using external respiratory signals acquired during respiratory-gated carbon-ion beam treatment. The substantial amount of data in this analysis ensures the statistical reliability of the results. For respiratory cycle, a statistically significant difference was observed between lung and liver. For duty cycle, a statistically significant difference was observed between liver and any other anatomical site. Peak exhalation position was statistically significantly more stable than peak inhalation position, and intrafractional variation in exhalation was statistically significantly smaller than interfractional variation. While a monotonous increase or decrease in baseline drift was observed in several examples, no particular direction (increasing or decreasing) was observed with regard to the trend in baseline drift.

Respiratory pattern

Mean ± SD respiratory cycle in this study was 4.1 ± 1.4 s. This is similar to the results reported by previous studies based on the respiratory motion during thoracic or abdominal radiotherapy treatment: 3.6 ± 0.8 s by Seppenwoolde et al. [20], 3.79 ± 1.10 by Wu et al. [22], and 3.8 ± 0.8 s by Suh et al. [23]. Respiratory cycle was significantly different between patients in the supine and

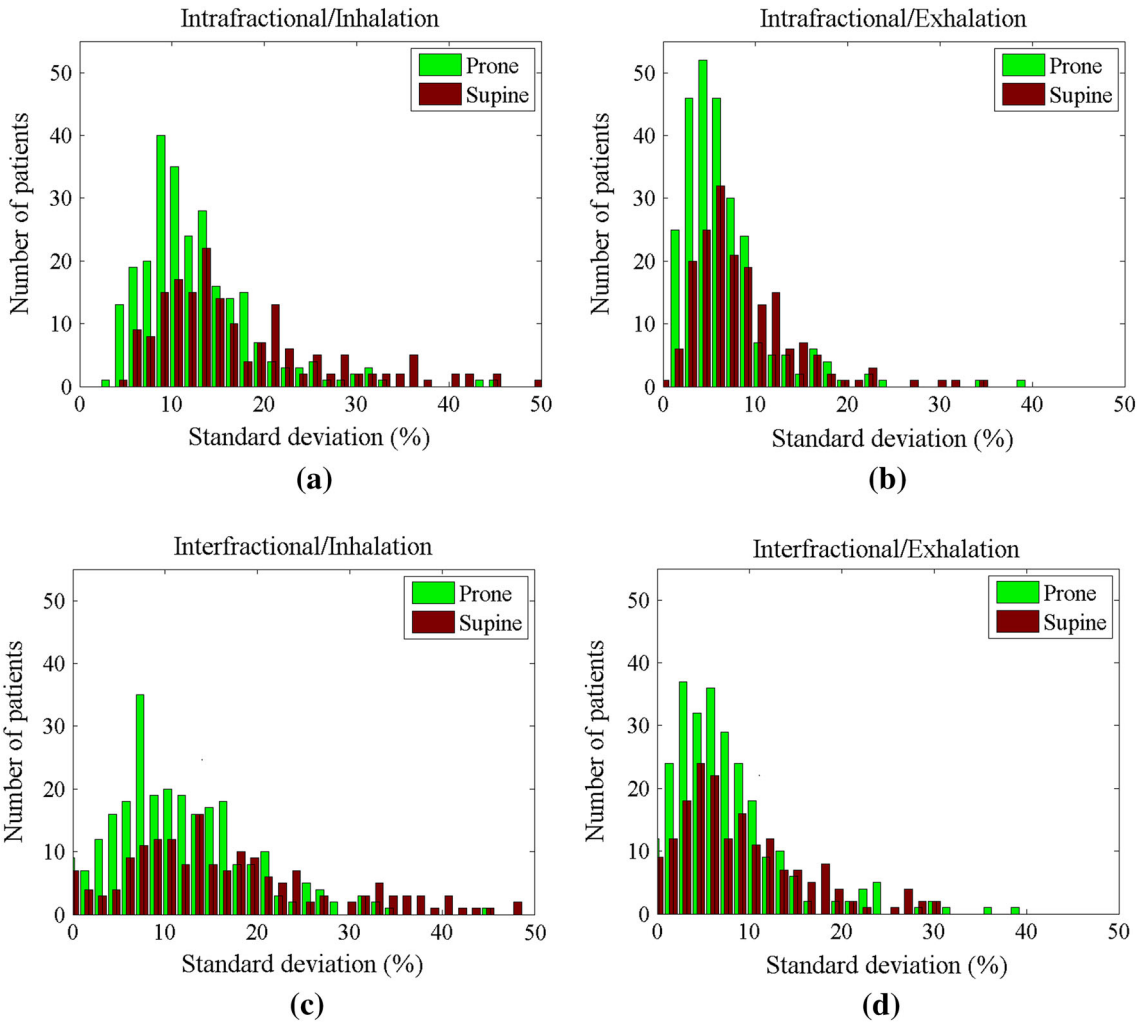

Fig. 8 Histograms of intrafractional variation (%) at **a** inhalation and **b** exhalation. Histograms of interfractional variation (%) at **c** inhalation and **d** exhalation

Table 3 Results for intrafractional and interfractional respiratory curve variations

	Phase	Total	Supine	Prone
Intrafractional variation (%)	Inhalation	15.5 ± 9.3	18.7 ± 12.4	13.0 ± 7.1
	Exhalation	7.5 ± 4.6	8.6 ± 5.6	6.6 ± 4.9
Interfractional variation (%)	Inhalation	17.2 ± 18.5	20.9 ± 24.6	12.6 ± 10.6
	Exhalation	9.4 ± 10.0	10.1 ± 12.7	7.7 ± 6.4

prone positions. In the present study, patients were immobilized to improve positional reproducibility. Since we have previously shown that immobilization tends to suppress the range of tumor motion [37], it might also affect the properties of the respiratory pattern, such as its stability. In the prone position, the patient's own weight suppresses inhalation, and this suppression might likely explain the shorter respiratory cycle in the prone than in the supine position.

With regard to duty cycle, typical beam duty cycle values during gated treatment vary between 30 and 50 % [38, 39]. Duty cycle in this study (= 37.5 ± 7.3 %) was within this range, because the therapist acted to maintain it against variation in respiratory pattern by adjusting the gating window.

With regard to baseline drift, the median of peak exhalation positions averaged in each 20-s block remained almost the same as that in the first time block, while the

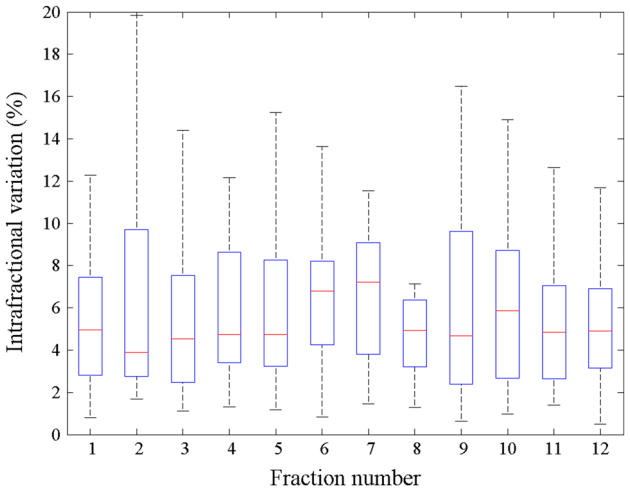

Fig. 9 Distribution of intrafractional variation as a function of fraction number in patients treated in 12 fractions. Intrafractional variation was defined by the standard deviation of peak exhalation position in each fraction. In the *box*-and-*whisker plot*, the central mark is the median, the edges of the *box* are the 25th and 75th percentiles, and the width of the whisker is chosen as four times the difference between the 25th and 75th percentiles. *Values* which lie outside the whisker are omitted

range of the distribution spread with time (Fig. 5). On the other hand, Zhao et al. reported that baseline drifted steadily with time toward the increasing (= inferior) direction over a large time scale (30 min) based on 51 lung SBRT treatments with Cyberknife Synchrony [24]. The reason for this discrepancy may be that the time scale of the treatment analyzed for baseline drift in the present study (2 min) was much shorter than that in Zhao's study. Further, their data were obtained using the correlation model integrated in the Cyberknife Synchrony, which calculates internal tumor motion from the external surface motion; and patients in our study were immobilized while those in Zhao's study were not.

With regard to variations in respiratory pattern, several reports have noted that these could be induced by various anatomic and physiologic factors [36, 40]. Although our medical staff attempt to make patients feel comfortable during treatment through verbal communication, most patients are nervous during the first few treatment fractions, including the CT scan and simulation processes, which might cause undesirable variation throughout the whole course of treatment. New treatment strategies which reduce variation in the patient's condition are therefore desirable.

Impact on dose conformation

Intra-/interfractional respiratory motion can affect dose conformity, and has been investigated in several studies in the photon [1] and particle therapy fields [3–5]. The most serious problem in respiratory pattern variation is respiratory amplitude variation.

Current treatment planning is usually based on a single respiratory cycle or a certain respiratory phase (generally peak exhalation), and a margin is added around the target so that the tumor receives an adequate dose. Presently, however, the size of this margin is determined without observation of tumor motion throughout the treatment course. Although no concrete strategy has yet been established, it is desirable that the extent of the margin be determined before treatment in a manner which takes proper account of respiratory pattern variation throughout the whole treatment. While 4DCT data via the acquisition of multiple respiratory cycles can provide a solution to this problem, consideration needs to be given to the very high patient dose it entails. Several studies have assessed the effects of respiratory motion on dose conformity in photon beam treatment using a computational phantom [41–43]. We are now developing a new methodology for estimating dose variation due to respiratory motion using multiple external respiratory cycle data and a computational phantom in carbon-ion beam treatment.

Improvement in respiratory stability

The human respiratory cycle is not strictly regular, but generally varies in amplitude and period from one cycle to the next, as seen in our results. Several approaches such as active breathing control (ABC) [44] and respiratory coaching [25, 39, 45] would likely improve respiratory variation.

Study limitations

Several limitations of this study warrant mention. First, the respiratory monitoring system used in this study provides the relative position of the surface marker only. We normalized the respiratory amplitudes by the amplitude of the first respiratory cycle in each fraction, rather than by the mean amplitude within the fraction, assuming that the first respiratory cycle represents a typical wave form since we started to record the respiratory wave just before irradiation after confirming that the respiratory pattern could be considered stable. It would be desirable if our system could have measured the amplitude in cm; however, the results obtained based on the phase information such as respiratory cycle and duty cycle still remain unchanged and the comparison of the variation is still valid even if we use relative amplitude. Second, we used respiratory data acquired using an external respiratory sensing monitor, which reflects motion of the patient's chest or abdominal surface. Although several studies have reported that the external marker represents internal motion [25–27], recent

studies have shown a discrepancy between external respiratory motion and internal tumor motion [28–33]. These studies were based on small populations, however, and further study is necessary, particularly with regard to accurate estimation of the impact of the discrepancy on dose conformity in a large population of patients. This is beyond the scope of the present study, however. Third, this study shows that the position of the exhalation peak varies by 7.5 ± 4.6 % in amplitude around the mean position of peak exhalation within a single fraction, and that the mean position of peak exhalation in a fraction also varies by 9.4 ± 10.0 % between fractions. Although this does not directly describe the variation in tumor motion itself, it does provide motivation for the observation of tumor motion using a monitoring system during treatment, such as fluoroscopy, and for irradiation of the treatment beam when the target is in a desirable position, rather than simply on the basis of respiratory phase. Even if the correlation between the external respiratory signal and tumor position is good, the respiratory pattern variation described here might induce under-dosing to the tumor when phase-based gating is used.

Conclusions

We quantified a large number of respiratory data obtained during respiratory-gated carbon-ion therapy and assessed their degree of variation. This information will aid the radiotherapy community in the planning of respiration management strategies. Consideration of intra-/interfractional respiratory variation in delivery of the treatment beam to the target will improve treatment accuracy.

Acknowledgments The authors wish to thank the clinical staff at the HIMAC of the National Institute of Radiological Sciences for their support.

Conflict of interest The authors declare no conflict of interest.

References

1. Bortfeld T, Jiang SB, Rietzel E (2004) Effects of motion on the total dose distribution. Semin Radiat Oncol 14(1):41–51
2. Juhler Nottrup T, Korreman SS, Pedersen AN et al (2007) Intra- and interfraction breathing variations during curative radiotherapy for lung cancer. Radiother Oncol 84(1):40–48
3. Furukawa T, Inaniwa T, Sato S et al (2007) Design study of a raster scanning system for moving target irradiation in heavy-ion radiotherapy. Med Phys 34(3):1085–1097
4. Mori S, Yanagi T, Hara R et al (2010) Comparison of respiratory-gated and respiratory-ungated planning in scattered carbon ion beam treatment of the pancreas using four-dimensional computed tomography. Int J Radiat Oncol Biol Phys 76(1):303–312
5. Mori S, Kanematsu N, Asakura H et al (2011) Four-dimensional lung treatment planning in layer-stacking carbon ion beam treatment: comparison of layer-stacking and conventional ungated/gated irradiation. Int J Radiat Oncol Biol Phys 80(2):597–607
6. Chen GT, Kung JH, Beaudette KP (2004) Artifacts in computed tomography scanning of moving objects. Semin Radiat Oncol 14(1):19–26
7. Mah D, Hanley J, Rosenzweig KE et al (2000) Technical aspects of the deep inspiration breath-hold technique in the treatment of thoracic cancer. Int J Radiat Oncol Biol Phys 48(4):1175–1185
8. Keall PJ, Joshi S, Vedam SS et al (2005) Four-dimensional radiotherapy planning for DMLC-based respiratory motion tracking. Med Phys 32(4):942–951
9. Keall PJ, Cattell H, Pokhrel D et al (2006) Geometric accuracy of a real-time target tracking system with dynamic multileaf collimator tracking system. Int J Radiat Oncol Biol Phys 65(5):1579–1584
10. D'Souza WD, Naqvi SA, Yu CX (2005) Real-time intra-fraction-motion tracking using the treatment couch: a feasibility study. Phys Med Biol 50(17):4021–4033
11. Shirato H, Shimizu S, Kitamura K et al (2000) Four-dimensional treatment planning and fluoroscopic real-time tumor tracking radiotherapy for moving tumor. Int J Radiat Oncol Biol Phys 48(2):435–442
12. Berbeco RI, Jiang SB, Sharp GC et al (2004) Integrated radiotherapy imaging system (IRIS): design considerations of tumour tracking with linac gantry-mounted diagnostic x-ray systems with flat-panel detectors. Phys Med Biol 49(2):243–255
13. Schweikard A, Shiomi H, Adler J (2004) Respiration tracking in radiosurgery. Med Phys 31(10):2738–2741
14. Mori S, Shirai T, Takei Y et al (2012) Patient handling system for carbon-ion beam scanning therapy. J Appl Clin Med Phys 13(6):3926
15. Rietzel E, Bert C (2010) Respiratory motion management in particle therapy. Med Phys 37(2):449–460
16. Bert C, Durante M (2011) Motion in radiotherapy: particle therapy. Phys Med Biol 56(16):R113–R144
17. Phillips MH, Pedroni E, Blattmann H et al (1992) Effects of respiratory motion on dose uniformity with a charged particle scanning method. Phys Med Biol 37(1):223–234
18. Minohara S, Kanai T, Endo M et al (2000) Respiratory gated irradiation system for heavy-ion radiotherapy. Int J Radiat Oncol Biol Phys 47(4):1097–1103
19. Keall PJ, Mageras GS, Balter JM et al (2006) The management of respiratory motion in radiation oncology report of AAPM Task Group 76. Med Phys 33(10):3874–3900
20. Seppenwoolde Y, Shirato H, Kitamura K et al (2002) Precise and real-time measurement of 3D tumor motion in lung due to breathing and heartbeat, measured during radiotherapy. Int J Radiat Oncol Biol Phys 53(4):822–834
21. Berbeco RI, Nishioka S, Shirato H et al (2005) Residual motion of lung tumours in gated radiotherapy with external respiratory surrogates. Phys Med Biol 50(16):3655–3667
22. Wu H, Sharp GC, Zhao Q et al (2007) Statistical analysis and correlation discovery of tumor respiratory motion. Phys Med Biol 52(16):4761–4774
23. Suh Y, Dieterich S, Cho B et al (2008) An analysis of thoracic and abdominal tumour motion for stereotactic body radiotherapy patients. Phys Med Biol 53(13):3623–3640
24. Zhao B, Yang Y, Li T et al (2011) Statistical analysis of target motion in gated lung stereotactic body radiation therapy. Phys Med Biol 56(5):1385–1395
25. Mageras GS, Yorke E, Rosenzweig K et al (2001) Fluoroscopic evaluation of diaphragmatic motion reduction with a respiratory gated radiotherapy system. J Appl Clin Med Phys 2(4):191–200
26. Vedam SS, Kini VR, Keall PJ et al (2003) Quantifying the predictability of diaphragm motion during respiration with a non-invasive external marker. Med Phys 30(4):505–513

27. Ahn S, Yi B, Suh Y et al (2004) A feasibility study on the prediction of tumour location in the lung from skin motion. Br J Radiol 77(919):588–596
28. Ozhasoglu C, Murphy MJ (2002) Issues in respiratory motion compensation during external-beam radiotherapy. Int J Radiat Oncol Biol Phys 52(5):1389–1399
29. Tsunashima Y, Sakae T, Shioyama Y et al (2004) Correlation between the respiratory waveform measured using a respiratory sensor and 3D tumor motion in gated radiotherapy. Int J Radiat Oncol Biol Phys 60(3):951–958
30. Hoisak JD, Sixel KE, Tirona R et al (2004) Correlation of lung tumor motion with external surrogate indicators of respiration. Int J Radiat Oncol Biol Phys 60(4):1298–1306
31. Ionascu D, Jiang SB, Nishioka S et al (2007) Internal-external correlation investigations of respiratory induced motion of lung tumors. Med Phys 34(10):3893–3903
32. Korreman SS, Juhler-Nottrup T, Boyer AL (2008) Respiratory gated beam delivery cannot facilitate margin reduction, unless combined with respiratory correlated image guidance. Radiother Oncol 86(1):61–68
33. Malinowski K, McAvoy TJ, George R et al (2012) Incidence of changes in respiration-induced tumor motion and its relationship with respiratory surrogates during individual treatment fractions. Int J Radiat Oncol Biol Phys 82(5):1665–1673
34. Mori S, Endo M, Komatsu S et al (2007) Four-dimensional measurement of lung tumor displacement using 256-multi-slice CT-scanner. Lung Cancer 56(1):59–67
35. Saw CB, Brandner E, Selvaraj R et al (2007) A review on the clinical implementation of respiratory-gated radiation therapy. Biomed Imaging Interv J 3(1):e40
36. Tobin MJ, Chadha TS, Jenouri G et al (1983) Breathing patterns. 1. Normal subjects. Chest 84(2):202–205
37. Dobashi S, Sugane T, Mori S et al (2011) Intrafractional respiratory motion for charged particle lung therapy with immobilization assessed by four-dimensional computed tomography. J Radiat Res 52(1):96–102
38. Ford EC, Mageras GS, Yorke E et al (2002) Evaluation of respiratory movement during gated radiotherapy using film and electronic portal imaging. Int J Radiat Oncol Biol Phys 52(2):522–531
39. Kubo HD, Wang L (2002) Introduction of audio gating to further reduce organ motion in breathing synchronized radiotherapy. Med Phys 29(3):345–350
40. Tobin MJ, Chadha TS, Jenouri G et al (1983) Breathing patterns. 2. Diseased subjects. Chest 84(3):286–294
41. Zhang J, Xu GX, Shi C et al (2008) Development of a geometry-based respiratory motion-simulating patient model for radiation treatment dosimetry. J Appl Clin Med Phys 9(1):2700
42. McGurk R, Seco J, Riboldi M et al (2010) Extension of the NCAT phantom for the investigation of intra-fraction respiratory motion in IMRT using 4D Monte Carlo. Phys Med Biol 55(5):1475–1490
43. Guo B, Xu XG, Shi C (2011) Real time 4D IMRT treatment planning based on a dynamic virtual patient model: proof of concept. Med Phys 38(5):2639–2650
44. Wong JW, Sharpe MB, Jaffray DA et al (1999) The use of active breathing control (ABC) to reduce margin for breathing motion. Int J Radiat Oncol Biol Phys 44(4):911–919
45. George R, Chung TD, Vedam SS et al (2006) Audio-visual biofeedback for respiratory-gated radiotherapy: impact of audio instruction and audio-visual biofeedback on respiratory-gated radiotherapy. Int J Radiat Oncol Biol Phys 65(3):924–933